Journal of Network Intelligence
Taiwan Ubiquitous Information
 ISSN 2414-8105 (Online)
Volume **6**, Number **4**, November **2021**

Measurement Optimization of Power Tower Based on Tilt Photography and Laser Scanning under Extreme Lighting Conditions

Zhijun Lin[1], Bin Xia [1*], Hongyang Zhang[1], Haomin Zhang [1] and Shiqiang Pang[2]

[1]Jiangmen Power Supply Bureau of Guangdong Power Grid Co. Ltd
Jiangmen, 529000, China

[2]Jiangmen Electric Power Design Institute Co., Ltd
Jiangmen, 529000, China

*Corresponding Author: 32672849@qq.com

Received June 2021; revised August 2021

Abstract. *The measurement of power line crossing on top of a power tower has always been a hindrance for the construction and maintenance of power tower, since the extreme lighting conditions in working environment has serious influence to the measurement instruments. The combination of Tilt Photography with Unmanned Aerial Vehicle (TP-UAV) and 3D laser scanning system offers an effective means of measuring the power line crossing. However, some of the measurement data cannot be recorded due to extreme lighting conditions, leading to inaccurate measurement. The missing data can be estimated using the recorded data based on an optimized high-dimensional error function. This paper introduces an improved artificial bee colony algorithm for the optimization of this error function, and the experimental results show that the missing data can be partially recovered to significantly improve the measurement accuracy of the two systems.*
Keywords: Tilted Photography, 3D laser scanning, UAV, deformation of tower

1. **Introduction.** Tilt Photography with Unmanned Aerial Vehicle (TP-UAV) technology is a system to carry out tilt photography on a UAV unit. This is mainly used in the geographic survey industry when the terrain of measurement is too complex to install measurement equipments [1–4]. The TP-UAV is a convenient way of measuring three-dimensional (3D) objects with the accuracy up to 20mm, and it can accurately measure the shape of a power tower or power line crossing. The best advantage of the TP-UAV is that it can record the object image in real time while measuring its 3D coordinates. 3D laser scanning system is a point cloud based measurement system installed on ground to provide millimeter level accuracy of 3D measurement for geographical survey industry. The advantage of the 3D laser scanning technique is the precision. The TP-UAV and the 3D laser scanning are two different technologies which show different performance in applications of geographic survey industry.

Although the accuracy of 3D laser scanning is higher than that of the TP-UAV, in real world industry applications, the terrains environment around the power lines are too complex to install a 3D scanning system on the ground. Also, the cost of the 3D laser scanning system is much higher than the TP-UAV and the efficiency is relatively lower. These shortcomings have limited the application of 3D laser scanning technology, and therefore in practical applications, 3D laser scanning systems are generally used with

the assistance of TP-UAV. In some typical applications for example, 3D laser scanning system is used as a calibration tool for the TP-UAV, offering an efficient way of measuring the deformation of high-voltage transmission facilities. In the combination of the two technologies, the measurement data based on the 3D laser scanning system is used to calibrate the measurement data of the TP-UAV through the least square solution, so as to correct the system error of the parameters and improve the measurement accuracy.

The combination of 3D laser scanning and TP-UAV can solve the problem of rapid and accurate measurement of obvious objects such as power tower. However, the measurement of line crossing is still limited, because the recording of power lines is more easily affected by lighting conditions, and therefore the data from some key measurement points will be missing. For example, in the case of strong light condition, some key measurement points will be overexposed, and therefore a series of maximum constants are recorded by the TP-UAV system. While under low illumination conditions, some key measurement points will be underexposed, and a series of zero constants will be recorded. Both cases would lead to failure measurement or decrease in accuracy. If some of the missing data cannot be measured directly, it is possible to approximate them by using computational models.

This paper introduces an approach to estimate the missing data due to extreme illumination conditions by using an optimization algorithm, so as to improve the accuracy of measurement. Since the missing parts of data are unpredictable in space, it is difficult to estimate their values accurately and the confidence intervals or variances are not possible to obtain. In order to overcome these problems, this research considers a measurement data estimation scheme using optimization methods such as the Parallel Compact Artificial Bee Colony (PCABC) to find the positions of points missed by the TP-UAV measurement system. Optimization algorithms are usually used to solve various nonlinear and non-differentiable mathematical problems. However, the missing measurement data caused by extreme illumination conditions generates a non-differentiable data space, and therefore it cannot be resumed by using recursive methods. Instead, the missing data can be approximated by the known parameters recorded by other means, and the parameters can be optimized to approach the true measurement data with a confidence interval.

The rest of the paper is organized as follows. The second part introduces the related work of optimization theory. The third section demonstrates the principle of power line crossing measurement based on the combination of 3D laser scanning and TP-UAV systems, and the experiment of using optimization algorithm to recover the missing measurement data are also presented. Finally in section 4, a conclusion is drawn.

2. **Related Work.** The ABC algorithm simulates the foraging behavior of bee colony, and uses swarm intelligence model to effectively solve complex optimization problems [5–8]. The ABC algorithm includes four basic elements: food source, employed bee, onlooker and scout. Food source is the solution of the optimization problem whose value represents the fitness of optimization. In the optimization process, the number of employed bees is equal to the number of food sources. When the bees find the food source information, they will share it with each other. The shared value is calculated with a probability function representing the degree of optimization and all other bees will decide which food source to choose. Onlookers choose food sources according to the food amount of all the employed bees in the hive area, while the scouts search for new food source near the hive. In the process of looking for new food sources, the bees will choose the strategy according to the information provided by the employed bees. If the amount food of a source has not been increased after a certain number of iterations, this source will be disregarded and the employed bees with the food source will become a scout and start to search for the next new food source.

The ABC method has been widely used in multi-objective optimization problems [9–12], but in many industrial applications, this algorithm often requires a high-performance computer to process and store a large amount of data. However, in field measurement of power lines crossing, high performance computing environment is hardly available, and therefore a Compact Evolutionary Algorithm (CEA) scheme was introduced for this purpose [13–15]. There is only one initial variable in the CEA algorithm and a number of iterations take place before reaching an optimal solution. Since there is only one variable involved, the CEA algorithm takes less memory to compute an optimization task and the computational load can be greatly reduced [16, 17]. Another Compact ABC (CABC) algorithm can not only reduce the memory occupancy, but also improve the convergence speed [18]. However, the CABC scheme can only produce one solution during each iteration with very low optimization efficiency, and the stability of the solution cannot be guaranteed. Therefore, when measuring the power line crossing, an improved multi-colony parallel CABC scheme can be introduced for the optimal estimation of missing data when encountering extreme lighting conditions. In this scheme, the optimization process is divided into several groups, each of which communicates with each other through certain strategies and protocols. After a certain number of iterations all the solutions will merge to the same solution, which is the final solution for the optimization process.

The optimal estimation of missing data in power line crossing measurement is a high-dimensional, multi-constraints and nonlinear problem, and only a few related literatures can be found. The difficulty of this optimization problem is to find the optimal solution quickly and accurately under multiple constraints. Among other optimization algorithms, the IB-RBCO algorithm can be used to solve UC and economic load distribution problems [19]. In the process of optimization, the ABC algorithm can also be applied with new mutation strategies to look for a larger food area, preventing individual repeated failed evolution and improving efficiency and convergence speed [20]. However, because the ABC strategy rarely considers the data storage as well as computational load at the same time, these optimization algorithms are not suitable for the recovery of TP-UAV measurement data. Therefore in field environment, a multi-core processor implemented with a parallel strategy is a suitable way to improve the optimization task. An example of two parallel solutions communicating with each other during optimization achieves better performance than just one [21, 22]. Another parallel strategy was proposed with a shared memory and multiprocessor scheme to improve the optimization efficiency [23]. Therefore, this study applies a Parallel and Compact ABC (PCABC) method to improve the efficiency, stability and reliability of the data estimation.

3. **Theory and methodology.**

3.1. **The measurement with TP-UAV calibrated with 3D laser scanning.**

In order to take the advantages of the accuracy of 3D laser scanning system and the convenience of the TP-UAV, these two technologies can be combined to achieve better performance. Practically, a one-off calibration process is required to find the projection coefficients of the measurement data from the two systems. In this application, a power line crossing is firstly measured with the 3D laser scanning system, and then the TP-UAV carries out several measurements to the line crossing. A set of least square coefficients is then calculated to represent the measurement data of the 3D scanning with the data sets from the TP-UAV. These least square coefficients become the calibration solution for the future measurement of the TP-UAV.

Since the data format of the 3D scanning system does not match that of the TP-UAV, a data conversion process is needed in order to unify the measurement coordinate and data

representation. In this study, the Bursa model is applied to convert the measurement data from the 3D laser scanning system to the coordinate of the TP-UAV system, such that,

$$\begin{pmatrix} X \\ Y \\ Z \end{pmatrix} = \begin{pmatrix} x_0 \\ y_0 \\ z_0 \end{pmatrix} + (1+\mu) \begin{pmatrix} \alpha X\prime \\ \beta Y\prime \\ \gamma Z\prime \end{pmatrix} \tag{1}$$

Where, $(X'\ Y'\ Z')^T$ is the 3D coordinate recorded by the 3D scanning system, and $(X\ Y\ Z)^T$ is the corresponding coordinate in the TP-UAV system. The Bursa model has seven parameters such as $(x_0\ \ y_0\ \ z_0\ \ \mu\ \ \alpha\ \ \beta\ \ \chi)$, where $(x_0\ \ y_0\ \ z_0)$ are the coordinate translation coefficients, μ is the scale factor, and $(\alpha\ \ \beta\ \ \chi)$ are the angle coefficients respectively. These coefficients are determined by manually measuring seven different calibration points on the power line crossing with both systems and solving the equations.

If there are L measurement points on the power line crossing and their positions from left to right and front to back are represented by $(X_j\ Y_j\ Z_j)^T$, where $(j = 1, 2, \ldots, L)$, for convenience of calculation, the three components of all the positions are expanded to form a vector such that,

$$u_i = (X_1^x\ Y_1^x\ Z_1^x\ X_2^x\ Y_2^x\ Z_2^x\ \cdots X_L^x\ Y_L^x\ Z_L^x)^T \tag{2}$$

where u_i denotes the ith time's measurement of the whole power line crossing by the TP-UAV system, and it is assumed that n times' measurement have been recorded such that $u_1, u_2, \ldots, u_n$. In the same way, the measurement data with the 3D laser scanning system can be written as,

$$v\prime = \left(X_1^{y\prime}\ Y_1^{y\prime}\ Z_1^{y\prime}\ X_2^{y\prime}\ Y_2^{y\prime}\ Z_2^{y\prime}\ \cdots X_L^{y\prime}\ Y_L^{y\prime}\ Z_L^{y\prime}\right)^T \tag{3}$$

and this measurement is usually carried out only once for calibration purpose. By converting v' into v, which is the coordinate of the TP-UAV with the Bursa model, it can be used for the calibration of the measurement data, such that,

$$v = (X_1^y\ Y_1^y\ Z_1^y\ X_2^y\ Y_2^y\ Z_2^y\ \cdots X_L^y\ Y_L^y\ Z_L^y)^T \tag{4}$$

The calibration of the TP-UAV data based on the 3D laser scanning system is through a least square solution of a linear representation [24]. The n times' measurement data from the TP-UAV such as $u_1, u_2, \ldots, u_n$, are formed a dataset to represent v obtained from the 3D laser scanning system such that,

$$v = a_1u_1 + a_2u_2 + \ldots + a_nu_n \tag{5}$$

where $a_i(i = 1, 2, \ldots, n)$ is the coefficient for each measurement u_i, and the vector operation form of Equation 5 can be written as,

$$U = VA \tag{6}$$

where $A = [a_1 \ldots a_n]^T, U = [u_1 \ldots u_n]^T.u_1 \ldots u_n$ and v are all column vectors. In case V is a nonsingular square matrix, the solution of Eq.(6) is given as,

$$A = U^{-1}.v \tag{7}$$

And if X is singular, A can be obtained by,

$$A = (U^TU + \mu I)^{-1}.U^Tv \tag{8}$$

where μ is a positive constant with small enough value and I is the identity matrix. In this way, when this calibrated TP-UAV system is applied to other power line crossing, it is generally required to carry out n times' measurement and the recorded data set is corrected to generate a measurement output by using Equation (6). It is assumed that if

the n times of measurement are performed properly by the TP-UAV system, all ui should be similar to each other, resulting in all the coefficients in A are close to identical.

In case of extreme lighting conditions, some parts of the measurement data in U will reach the maximum value in overexposure situation and minimum value in low light condition. If some groups of element in u_i all present constant extreme values, they will be identified as missing recordings. If the jth element of ui is missing, it can be denoted as $u_{ij}(j \in \Phi)$ where Φ is the set of labels corresponding to each of the missing elements and $j = 1, 2, \ldots, 3L$. An error function can be designed as

$$erf(\Phi) = \sum_{i} \left(\sum_{j \in \Phi} a_i u_{ij} - \sum_{j \notin \Phi} a_i u_{ij} \right) \tag{9}$$

which represents the difference of the sum of the missing coordinates and the corresponding recorded coordinates in other measurements multiplied by the respective coefficient. The variables of the error function in Equation 9 are the missing coordinates, and the minimization solution of Equation 9 will give rise to an approximation of the missing data that fit the least square solution in Equation 7 or 8.

3.2. **Optimization with the parallel and compact strategy.** In this study, the optimization of the error function in Equation 9 is performed using a PCABC scheme. The recorded coordinate data by the TP-UAV system is generally regarded as following a normal distribution, which can be used for the modeling of the solution. In the parallel and compact scheme, several initial solutions are setup as the starting points, each of which is represented by an employed bee. The distribution of each employed bee is modeled by a truncated Probability Distribution Function (PDF) following the Gaussian distribution with a mean value of μ and a standard deviation of δ [25]. The solution of this scheme is modeled by a Probability Vector (PV) [26]. In this measurement data approximation task, it is assumed that there are m elements in the set of Φ, therefore there are $2 \times m$ elements in the matrix vector of PV such that,

$$PV^t = \left[\mu^t, \delta^t\right] \tag{10}$$

where t is the iteration step and the value of the PDF is normalized so that the total probability is limited to one. The solution of U can be represented by $PV\left(\mu_i, \delta_i\right)$, where $i = 1, 2, \ldots, m$ and the corresponding PDF is given as [27],

$$PDF_{\mu_i,\sigma_i}(\Phi) = \frac{e^{-\frac{(\Phi-\mu_i)^2}{2\delta_i^2}} \sqrt{\frac{2}{\pi}}}{\delta_i \left(erf\left(\frac{u_i+1}{\sqrt{2}\delta_i}\right) - erf\left(\frac{u_i-1}{\sqrt{2}\delta_i}\right)\right)} \tag{11}$$

The resulting Cumulative Distribution Function (CDF) is given by the Chebyshev polynomials such that [28]

$$CDF = \int_0^1 \frac{e^{-\frac{(-\mu_i)^2}{2\delta_i^2}}}{\delta_i(erf(\frac{\mu_i+1}{\sqrt{2}\delta_i}) - \mathrm{erf}(\frac{\mu_i-1}{\sqrt{2}\delta_i}))} d\Phi \tag{12}$$

The optimized solution of Φ can be obtained by calculating the inverse function of the CDF. The initial values of μ and δ are set to 0 and 10 respectively. In the process of optimization, the value of Φ is updated to another position where the error function is evaluated, and the solution with a relatively smaller value is called a winner position,

otherwise is a loser position. The values of μ_i and δ_i are also updated accordingly such that,

$$\mu_i^{t+1} = \mu_i^t + \frac{1}{N_p}(\text{ winner }_i - \text{ loser }_i) \tag{13}$$

$$\delta_i^{t+1} = \sqrt{(\delta_i^t)^2 + (\mu_i^t)^2 - (\mu_i^{t+1})^2 + \frac{(\text{ winner }_i^2 - loser_i^2)}{Np}} \tag{14}$$

It is noted that the values of the element in the variable set Φ are bounded by the minimum and maximum recorded values of the TP-UAV system, therefore a constraint must be applied to the optimization process such that,

$$U_{min} \leq u_{ij} \leq U_{max} \tag{15}$$

where U_{min} and U_{max} are the lower limit and upper limit of the recording value of the TP-UAV system respectively.

The optimization steps with the PCABC algorithm to find a minimum solution for Equation 9 are given as:

1. Supposed that the number of processors is R, there will be R groups of PV solution being initialized;
2. Each group selects an elite based on the ABC algorithm;
3. In the next iteration, the value of the error function produced by each of the group is compared with that of the previous elite, and keep the better one to update the PV;
4. After a certain number of iterations, each of the groups communicates with each other and find the best solution to replace the elites of all groups, and the corresponding PVs are also replaced;
5. Repeat $1 \sim 4$ steps until the termination conditions are satisfied.

3.3. **Experiment with industry applications.** In order to demonstrate the performance of the proposed method, a power tower of about 70m high carrying multi-loop high voltage of 220 kV transmission lines is measured with both the TP-UAV and 3D laser scanning systems. The power tower was built in a rural area with subtropical forests growing on different geological structures like mountains, and therefore the lighting conditions of the environment are complicated and unpredictable. The sunlight condition around the power tower can also be influenced by the existing power line networks and other projects under construction, making it more difficult for a measurement task. Figure 1 and Figure 2 show two typical point cloud images of the data measured by a 3D laser scanning system and a TP-UAV system above the air respectively.

3.4. **Watermark embedding phase.**

For demonstration purpose, this power tower and the line crossing are measured with both the 3D laser scanning system and the TP-UAV system under both overexposure and underexposure conditions. Table 1 shows the coordinates of 13 measurement points recorded by the both systems under a perfect lighting condition, and the measurement data recorded by the 3D laser scanning system has been converted to the coordinate of the TP-UAV system through Equation 1. The origin of the XY coordinates is based on the power tower where the power lines start about 60km away, and the origin of the height (Z coordinate) is based on the ground of the power tower. The measurement data recorded by the TP-UAV system has been calibrated by the 3D laser scanning system. It can be seen that the maximum systematic error of the TP-UAV system from the 3D laser scanning system is about 22mm with the average of about 12mm. The measurement accuracy of the TP-UAV system can well satisfy the requirement of the power line and tower measurement, which must be less than 50mm.

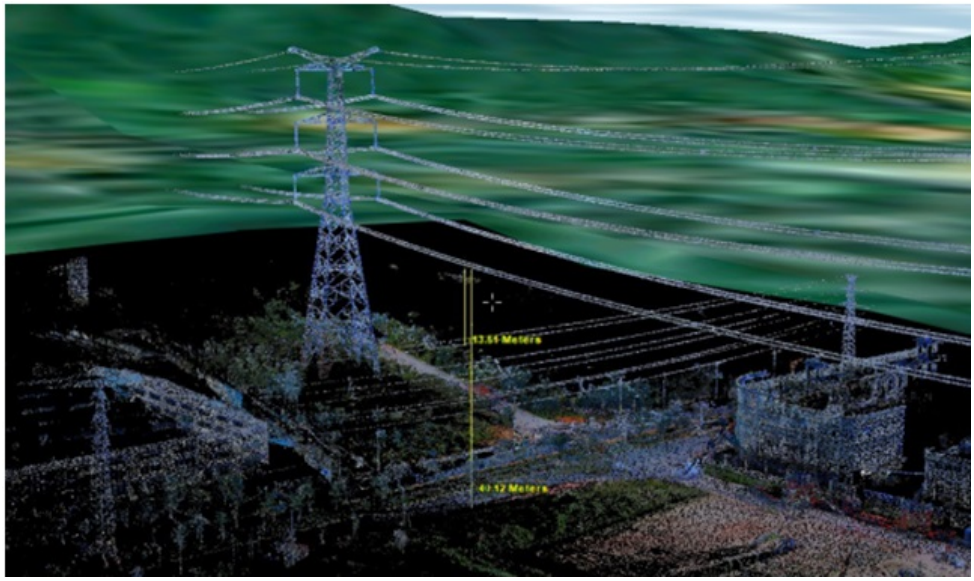

FIGURE 1. The point cloud image of one of the towers measured by the TP-UAV system above the air..

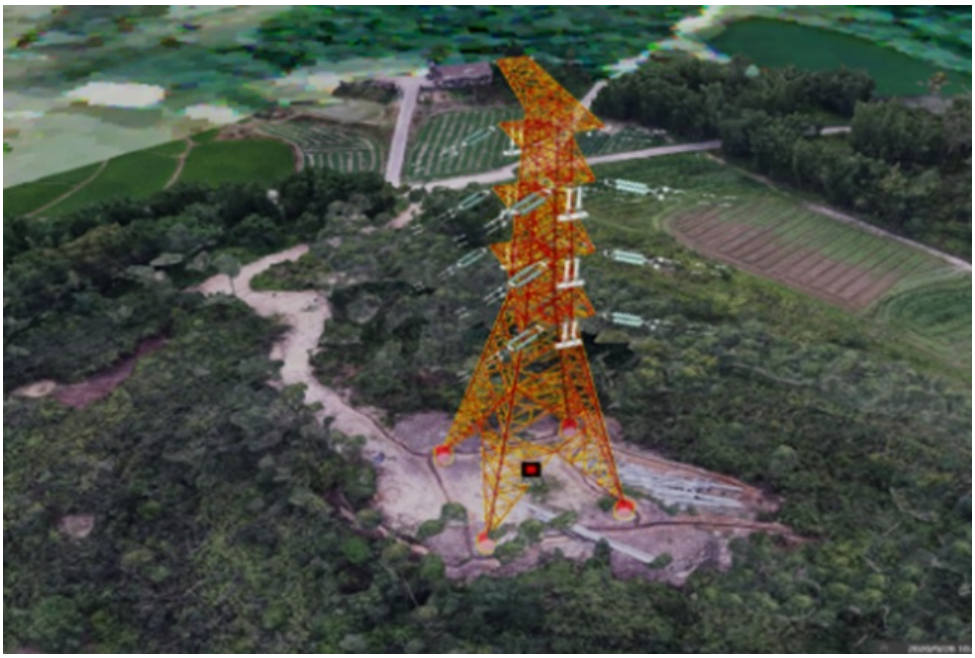

FIGURE 2. The point cloud image of one of the towers measured by the 3D scanning system..

In the experiment the performance of the TP-UAV system is also tested under extreme lighting conditions such as overexposure and underexposure. The TP-UAV system recorded a set of data during daytime when the sunlight is the strongest, leading to overexposure of the recording camera. Figure 3(a) shows the point cloud image of a power tower with 25000 measurement points recorded by the TP-UAV system under strong light condition, and it can be seen that only 3658 points can be used as valid measurement data for 3D reconstruction, accounting for only 14.63% of the total measurement points. This valid recording rate under strong light environment is not acceptable for the 3D measurement of the power tower, which requires at least 50% valid recording of the coordinates.

TABLE 1. The comparison of measurement data from both the 3D laser scanning system and the TP-UAV system.

NO.	3D laser scanning system (m)			TP-UAV system (m)			Error (m)		
	X	Y	Z	x	y	z	Dx	Dy	Dz
1	32659.71	62922.242	66.616	32659.708	62922.247	66.605	-0.002	0.005	-0.011
2	42807.804	64663.308	72.891	42807.799	64663.306	72.869	-0.005	-0.003	-0.022
3	44881.183	85990.467	57.705	44881.19	85990.45	57.724	0.007	-0.017	0.019
4	49879.346	54628.685	52.897	49879.326	54628.679	52.895	-0.019	-0.006	-0.002
5	51569.381	68903.335	55.265	51569.365	68903.343	55.263	-0.016	0.008	-0.002
6	52650.06	72017.472	53.668	52650.048	72017.471	53.656	-0.012	0	-0.012
7	54060.021	57224.324	72.443	54060.008	57224.31	72.452	-0.013	-0.014	0.009
8	56349.928	60731.982	53.899	56349.923	60731.964	53.913	-0.005	-0.018	0.013
9	58106.627	48881.954	53.686	58106.63	48881.963	53.685	0.003	0.009	-0.001
10	59318.775	56961.722	53.58	59318.767	56961.735	53.588	-0.008	0.013	0.008
11	59630.219	72155.827	68.715	59630.219	72155.833	68.704	0	0.006	-0.011
12	60958.116	66376.951	56.609	60958.1	66376.945	56.623	-0.017	-0.006	0.014
13	63093.648	63034.477	54.266	63093.663	63034.488	54.255	0.016	0.011	-0.011

Figure 3(b) shows the point cloud image of this power tower using the proposed data approximation method, and it can be seen that up to 14562 valid points are available for 3D measurement. Through the proposed optimization scheme with the PCABC algorithm, the successful recording rate of the TP-UAV system under strong light condition can be increased up to 58.24%, which can be used for the 3D measurement of the power tower.

(a) The original recording with only 3658 valid points.

(b) The approximation recovery point cloud with 14562 valid points.

FIGURE 3. Point cloud images of a power tower with 25000 measurement points recorded by the TP-UAV system under strong light condition

During the night time when there is no sufficient light for the TP-UAV system to record measurement points, the proposed method can also be used for the recovery of missing data. Figure 4 (a) shows an point cloud image of another power tower with 20000 measurement points recorded by the TP-UAV system under dim light condition, however, there are only 3997 valid points available, and the valid rate is only 19.98%. Figure 4 (b) shows the point cloud image with the recovery data points and it can be seen that there are 16616 valid points obtained and the valid rate can go up to 83.08%, which is suitable for the 3D measurement of the power tower.

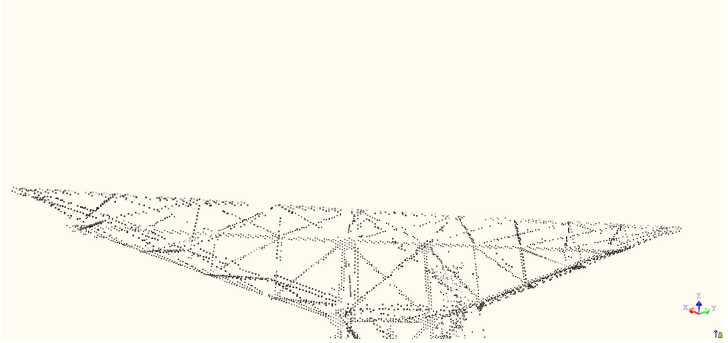

(a) The original recording with only 3997 valid points.

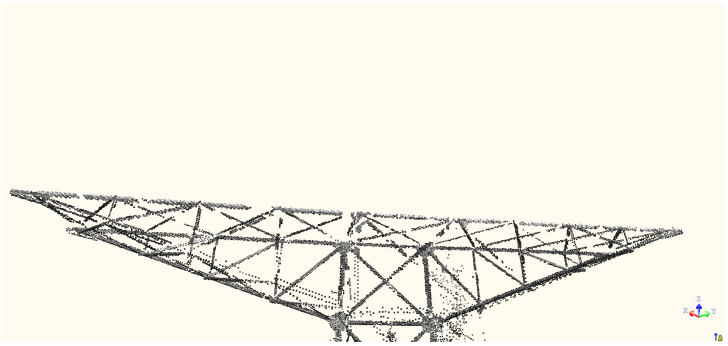

(b) The approximation recovery point cloud with 16616 valid points.

FIGURE 4. Point cloud images of a power tower with 20000 measurement points recorded by the TP-UAV system under dim light condition at night.

4. **Conclusion.** This paper presents a measurement data estimation scheme for the TP-UAV system to cope with the field recording under extreme lighting conditions. This measurement data estimation approach is based on an optimization scheme called the Parallel Compact ABC (PCABC) algorithm. The recorded coordinates of the TP-UAV system are firstly calibrated by a 3D laser scanning system, which is generally regarded as a measurement system with ground truth accuracy. Then the TP-UAV system carries on measurement on power lines and power towers. However, during the daytime when sunlight is strong, the camera on the TP-UAV system is overexposed and a considerable part of the points on the power lines or towers cannot be recorded. The same happens to the recording during the night or extreme weather condition when the target is too dim to record. It was shown in the experiment that under both extreme conditions, the missing measurement data can be partially estimated and recovered with the proposed method, improving about 30% of the measurement blind spots.

Acknowledgment. This research is funded by the New Science and Technology Funding of the Power Grid Ltd. of Guangdong Province, China under project No. 030700KK52180151.

REFERENCES

[1] Y. Qu, L. Jiang, X. Guo. Moving vehicle detection with convolutional networks in UAV videos, *2016 2nd International Conference on Control, Automation and Robotics (ICCAR)*, pp. 225-229, 2016.

[2] N. Šarlah, T. Podobnikar, T. Ambrožič, B. Mušič. Application of Kinematic GPR-TPS Model with High 3D Georeference Accuracy for Underground Utility Infrastructure Mapping: A Case Study from Urban Sites in Celje, Slovenia, *Remote Sensing*, vol.12, 1228, 2020.

[3] H. Cui, Z. Lin, J. Sun. Research on the 3D modeling method for remote sending images of big degree of overlap acquired by unmanned aerial vehicle, *Science of Surveying and Mapping*, Vol.30, no.2, pp.36-38, 2005.
[4] C. Tan, P. Li, L. Wen, C. Pan, Improvement of 3D urban modeling method based on unmanned aerial vehicle photography. *Bulletin of Surveying and Mapping,* vol.11, pp. 39-42, 2016.
[5] S. Jadon, R. Tiwari, H. Sharma, J. Bansal, Hybrid artificial bee colony algorithm with differential evolution, *Applied Soft Computing*, vol. 58, pp.11-24, 2017.
[6] B. Akay, D. Karaboga, Artificial bee colony algorithm for large-scale problems and engineering design optimization, *Journal of intelligent manufacturing*, vol. 23, no. 4, pp. 1001-1014, 2012.
[7] M. Sonmez, Artificial Bee Colony algorithm for optimization of truss structures, *Applied Soft Computing*, vol. 11, no. 2, pp. 2406-2418, 2011.
[8] D. Karaboga, B. Basturk, On the performance of artificial bee colony (ABC) algorithm, *Applied soft computing*, vol. 8, no. 1, pp. 687-697, 2008.
[9] N. Taspinar, D. Karaboga, M. Yildirim, B. Akay, Partial transmit sequences based on artificial bee colony algorithm for peak-to-average power ratio reduction in multicarrier code division multiple access systems, *IET Communications*, vol. 5, no. 8, pp. 1155-1162, 2011.
[10] Z. Meng, J. Pan, L. Kong, Parameters with Adaptive Learning Mechanism (PALM) for the enhancement of Differential Evolution. *Knowledge-Based System*, vol. 141, pp. 92-112, 2018.
[11] T. Wu, Z.Y. Lee, L. Yang, C.M. Chen, A Provably Secure Authentication and Key Exchange Protocol in Vehicular Ad Hoc Networks", *Security and Communication Networks*, vol. 2021, 9944460, 17 pages, 2021.
[12] S. Chu, H. Huang, J. Roddick, J. Pan, Overview of Algorithms for Swarm Intelligence. Computational Collective Intelligence, Technologies and Applications (ICCCI 2011), *Lecture Notes in Computer Science*, vol. 6992, pp. 28-41, 2011.
[13] G. Zhou, H. Moayedi, M. Bahiraei, Z. Lyu. Employing artificial bee colony and particle swarm techniques for optimizing a neural network in prediction of heating and cooling loads of residential buildings, *Journal of Cleaner Production*, vol. 254, 120082, 2020.
[14] M. Bijandi, M. Karimi, B. Bansouleh, Agricultural land partitioning model based on irrigation efficiency using a multi-objective artificial bee colony algorithm, *Transactions in GIS*, vol. 25, pp. 551-574, 2021.
[15] A. Tian, S. Chu, J. Pan, H. Cui, W. Zheng, A Compact Pigeon-Inspired Optimization for Maximum Short-Term Generation Mode in Cascade Hydroelectric Power Station, *Sustainability*, vol. 12, no. 3, 767, 2020.
[16] Z. Gu, Y. Zhu, Y. Wang, X. Du, M. Guizani, Z. Tian, Applying artificial bee colony algorithm to the multiplot vehicle routing problem, *Software Practice and Experience*, https://doi.org/10.1002/spe.2838 , 2020.
[17] J. Pan, P. Hu, S. Chu, Novel Parallel Heterogeneous Meta-Heuristic and Its Communication Strategies for the Prediction of Wind Power, *Processes*, vol. 7, no. 11, 845, 2019.
[18] T. Dao, S. Chu, T Nguyen, C. Shieh, M. Horng, Compact artificial bee colony, *The 27th International Conference on Industrial Engineering and Other Applications of Applied Intelligent Systems (IEA/AIE 2014)*, pp. 96-105, 2014.
[19] P. Lu, J. Zhou, C. Wang, Q. Qiao, L. Mo. Short-term hydro generation scheduling of Xiluodu and Xiangjiaba cascade hydropower stations using improved binary-real coded bee colony optimization algorithm, *Energy Conversion and Management*, vol. 91, pp. 19-31, 2015.
[20] X. Wen, J. Zhou, Z. He, C. Wang, Long-term scheduling of large-scale cascade hydropower plants using improved differential evolution algorithm, *Water*, vol. 10, no. 4, 383, 2018.
[21] X. Sui, S. Chu, J. Pan, H. Luo. Parallel Compact Differential Evolution for Optimization Applied to Image Segmentation, *Applied Sciences*, vol. 10, no. 6, 2195, 2020.
[22] L. Kang, R. Chen, N. Xiong, Y. Chen, Y. Hu, C. Chen, Selecting Hyper-Parameters of Gaussian Process Regression Based on Non-Inertial Particle Swarm Optimization in Internet of Things, *IEEE Access*, vol. 7, pp. 59504-59513, 2019.
[23] D. Abramson, J. Abela, A parallel genetic algorithm for solving the school timetabling problem, *Division of Information Technology*, CSIRO, 1991.
[24] Y. Xu, D. Zhang, J. Yang, J. Yang, A Two-Phase Test Sample Sparse Representation Method for Use With Face Recognition, *IEEE Transactions on Circuits and Systems for Video Technology*, vol. 21, no. 9, pp. 1255-1262, 2011.

[25] M. Younis, M. Youssef, K. Arisha, Energy-aware routing in cluster-based sensor networks, In Proceedings, *The 10th IEEE international symposium on modeling, analysis and simulation of computer and telecommunications systems*, pp.129-136, 2002.

[26] J. Chang, S. Chu, J. Roddick, J. Pan, A Parallel Particle Swarm Optimization Algorithm with Communication Strategies, *Journal of Information Science and Engineering*, vol. 21, pp. 809-818, 2005.

[27] W. Gautschi, Error function and Fresnel integrals, *Handbook of Mathematical Functions*, vol. 55, pp.297-308, 1972.

[28] R. Pemantle, A survey of random processes with reinforcement, *Probability Surveys*, vol. 4, no. 25, pp. 1-79, 2007.